2020 IEEE/RSJ International Conference on Intelligent Robots and Systems (IROS)
October 25-29, 2020, Las Vegas, NV, USA (Virtual)

Friction Identification in a Pneumatic Gripper

Rocco A. Romeo[1], Marco Maggiali[1], Daniele Pucci and Luca Fiorio[1]

***Abstract*— Mechanical systems are typically composed of a number of contacting surfaces that move against each other. Such surfaces are subject to friction forces. These dissipate part of the actuation energy and cause an undesired effect on the overall system functioning. Therefore, a suitable model of friction is needed to elide its action. The choice of such a model is not always straightforward, as it is influenced by the system properties and dynamics. In this paper, we show the identification of different friction models and evaluate their prediction capability on an experimental dataset. Despite being state-of-the-art models, some modifications were introduced to improve their performance. A pneumatic gripper was used to collect the data for the models evaluation. Two experimental setups were mounted to execute the experiments: information from two pressure sensors, a load cell and a position sensor was employed for the identification. During the experiments, the gripper was actuated at different constant velocities. Results indicate that all the identified models offer a proper prediction of the real friction force.**

I. INTRODUCTION

Friction is a fundamental quantity to be accounted for in mechanical engineering. It usually degrades the behavior of physical systems and, depending on the complexity of such systems, might complicate the design of control algorithms. Despite its effect is mitigable by means of lubricant films with a certain thickness, a proper model of friction is always required to effectively compensate for such an effect. Nonetheless, friction is quite difficult to model; this is known since several decades [1]. A number of models, characterized by varying complexity, were proposed so far. Among the classical ones, there is the Coulomb model, which dates back to more than two centuries ago. According to this model, when one surface slides over another one, the friction force F_{fd} is proportional to the applied normal force F_n through a constant, namely kinetic coefficient of friction μ_d. When there is no sliding, the friction force can be as high as a value $F_{fs} = \mu_s F_n$, with $\mu_s > \mu_d$. This phenomenon is known as stiction. In all cases, the sign of the sliding velocity has to be involved in the friction force computation. When the system exhibits a certain degree of viscosity, i.e. friction force grows along with velocity $\dot{x}$, a further term can be added in the form $\mu_v \dot{x}$, being μ_v the viscous coefficient.

Thanks to its simplicity, the Coulomb model was largely employed in physics and engineering, and its usage is still quite common [2]. In general, simple models such as the Coulomb's one are easier to implement but they do not capture all the frictions phenomena, such as stick-slip. Moreover, when there is no movement between two contacting surfaces, the Coulomb's model cannot predict friction.

[1]iCub Tech, Istituto Italiano di Tecnologia, Via San Quirico 19D, 16163 Genoa, Italy. Email: firstname.lastname@iit.it

To achieve higher detail, effects such as the Stribeck one are to be considered. A similar effect takes into account the aforementioned stick-slip [3], which occurs at low velocities and causes a non-linear drop in the friction force. Typically, the expression of the Stribeck phenomenon features an exponential function. Despite its greater completeness, even the Stribeck model does not resolve the discontinuity at null velocity introduced by the Coulomb model.

In this paper, we intend to identify one or more suitable friction models for a real mechanical system, i.e. a pneumatic gripper. Even though there exist more complex compensation techniques (e.g. [4], in this initial study we concentrate on model-based approaches. Four models will be first identified and then evaluated, namely: Coulomb model with viscous friction (CV), Karnopp model [5], Threlfall model [6], and the Coulomb model with viscous friction and Stribeck effect (CVS). The models were selected based on their variegated characteristics: most probably, the highest degree of detail is provided by the CVS model which combines the Coulomb and viscous friction, along with the non-linearity typical of stick-slip. Some modifications were introduced to all the four models in order to remove the discontinuity at null velocity and/or to achieve superior performance. Notice that acronyms are given only for long names, i.e. only for CV and CVS models. It is also worth mentioning that all the selected models were static. i.e. they cannot work when $\dot{x}$ is non-constant. Dynamic models such as LuGre [1] will be investigated in successive studies.

For all the models, the identification experiments were therefore conducted at constant velocity, on two different setups involving the gripper and two pressure regulators actuating it. Pneumatic grippers are still the most used in robotics [7], though friction was much more rarely investigated in these systems rather than e.g. in pneumatic cylinders [8]. Therefore, the aim of this study is to analyze friction forces in an off-the-shelf pneumatic gripper, providing insight on how such forces influence its functioning. Moreover, the understanding of friction would be of great help in the design of control strategies for pneumatic grippers, which still lack of reliable closed-loop force regulation [7]. In our previous works [7]-[9], we showed two force-control architectures that resorted to optimization algorithms [7], Kalman filters and state observers [9]. Nonetheless, the performance of such architectures was somehow limited by the lack of a friction model.

The rest of the paper is structured as follows: Section II shows the pneumatic gripper adopted and the experimental setups, whereas Section III presents the friction models, which are all static models. Section IV illustrates the identi-

fication procedure and the experimental tests, as well as the results. Finally, Section V concludes the article and gives some hints about the future work.

II. MATERIALS: PNEUMATIC GRIPPER AND EXPERIMENTAL SETUPS

This Section will present the employed device, i.e. the pneumatic gripper, which is the same as in our previous works [7]-[9]. Moreover, the chosen friction models will be described. The manufacturer of the gripper cannot be revealed due to disclosure restrictions. The two experimental setups will be shown as well.

A. Pneumatic Gripper

The pneumatic gripper was constructed and actuated following a classical architecture. It is possible to divide it into two subsystems. The first subsystem is the pneumatic one, while the second subsystem is the mechanical transmission. The pneumatic subsystem includes the entire pneumatic cylinder (piston and air chambers, whereas the mechanical subsystem includes the jaws, levers, and the section of the piston rod that resides out of the cylinder's chambers.

When the piston moves, it applies a force on the mechanical subsystem. This results into the actuation of the levers, and thus of the jaws on which custom fingers can be mounted (see next Section). Even though the levers rotate, the consequent displacement of the jaws is linear. Such a displacement is the most subject to friction forces, especially when the gripper is commanded to reopen (as shown in Section IV).

A representation of the gripper section is given in Fig. 1. by increasing the pressure in the closing chamber the piston moves down. On the contrary, by increasing the pressure in the opening chamber the piston moves up. The motion of the piston is converted into an opening/closing motion of the gripper jaws by two levers. The levers are constrained to the gripper main body by a pin joint. It is important to notice that the jaws movement is symmetric, so that a certain displacement d_1 of one jaw implies a displacement $-d1$ of the other jaw.

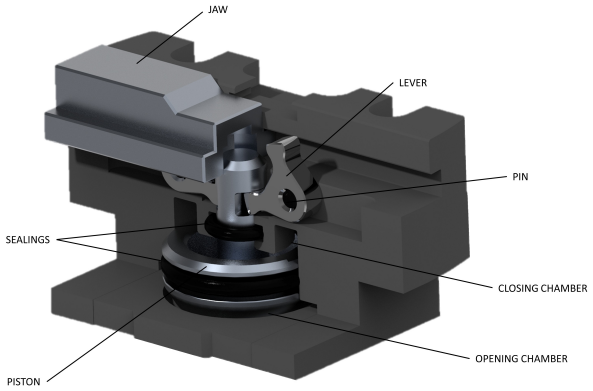

Fig. 1. Section of the pneumatic gripper [9]

Mathematically, it is necessary to consider that the force coming from the piston is divided by the number of fingers, i.e. of jaws. Indeed, the piston gives motion to all the levers connected to it. Being the gripper composed of two jaws, one has:

$$F_J = \frac{(F_o - F_c)}{2}. \tag{1}$$

where F_o and F_c denote the force contribution from the opening and closing chamber, respectively. Their difference is such that:

$$F_P = F_o - F_c. \tag{2}$$

Clearly, both forces F_o and F_c depend on the applied pressures P_o and P_c in the relevant chambers through the following formula:

$$F_{o|c} = P_{o|c} A_{o|c}, \tag{3}$$

where $A_{o|c}$ is the area of the opening or closing chamber, and $P_{o|c}$ is the associated pressure. The two pneumatic chambers have different areas; therefore, if both chambers are supplied with the same pressure $P_o = P_c$, the resulting forces F_o and F_c will not have the same magnitude. Part of F_P is dissipated due the friction generated between the jaws guides and the gripper body when the grasping force changes.

The gripper chambers were supplied by two micro-pressure regulators, one per chamber. Each regulator embedded a sensor which allowed measuring the pressure fed to the gripper chambers. More details about the experimental setups will be provided in the next Subsection.

B. Setups

To perform the identification experiments, two setups were conceived. In the first one (Fig. 2), namely *spring* setup, the gripper was instrumented with a pair of flat, L-shaped fingers, which were designed by means of a CAD software. The fingers were mounted on the jaws: the load cell was fixed on one of such fingers, to which a compression spring was interfaced. On the other side, the spring was connected to the remaining finger. Such a configuration allowed reproducing the grasping of an object with a certain stiffness (i.e. the spring stiffness). The described setup was already used in our previous work [7], but in the present study a laser sensor was added to measure the jaws position. During the experiments on this setup, the gripper was controlled through the closed-loop force control presented in [7] as well.

The second setup, namely *no-spring* setup, was constructed exactly as the first one except for the spring and load cell which were no longer present. The aim of this choice was to let the gripper move freely with a null stiffness between the fingers. Consequently, in this setup the gripper could not be controlled with the same force control used in the *spring* setup. Rather, a position control based on the laser sensor measurement was implemented. The position control used a

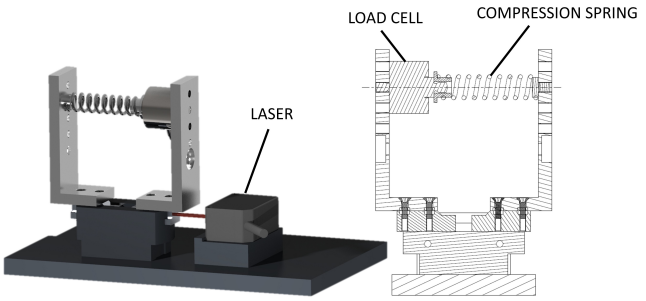

Fig. 2. CAD of the *spring* setup (on the left) with its section (on the right).

PID block to adjust the actual position of the jaws resorting to the feedback provided by the laser sensor.

Fig. 3 illustrates the pneumatic scheme adopted for the experiments. The gripper was actuated by the two pressure regulators, which were supplied by an air compressor. The electronics unit managed all the analog inputs and outputs. The inputs were: I) pressure measurements from the regulators sensors; II) force measurement from the load cell; III) position measurement from the laser sensor.

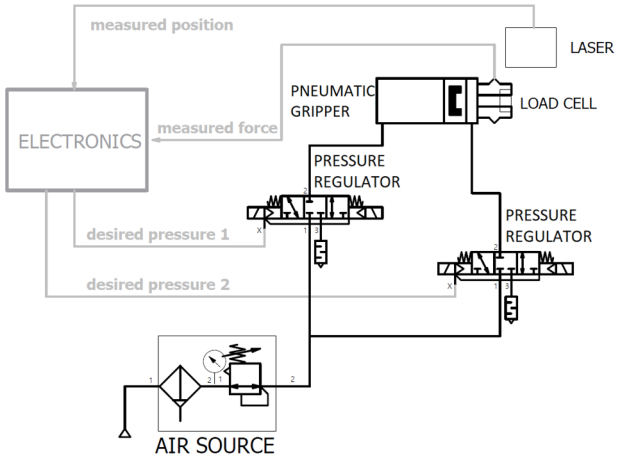

Fig. 3. Pneumatic scheme and connections.

The entire pneumatic system, along with all the sensors, was commanded through a LabVIEW program; the desired input for the regulators was generated at 1 kHz. Sensor data were collected at the same frequency. For this task, a connector block, namely NI SCB 68A, was interfaced to a NI 6251 data acquisition device.

III. Friction Models

Here, the four selected friction models will be briefly described. Modifications introduced in each model will also be detailed.

A. CV Model

The Coulomb friction model was probably the first one to be published in the scientific literature. Known for its simplicity, this model assumes that friction force F_f is linearly dependent on the normal force F_n applied onto a certain surface. The mathematical formulation is rather straightforward:

$$F_f = \begin{cases} \mu_d F_n \text{sign}(\dot{x}) + \mu_v \dot{x} & |\dot{x}| \neq 0 \\ \min(F, \mu_d F_n)\text{sign}(F) & |\dot{x}| = 0. \end{cases} \quad (4)$$

In (4), μ_d is the dynamic coefficient of friction and F is the resultant of all the forces acting on the surface, whereas μ_f is the coefficient of viscous friction. The value of F_f depends on the sign of the sliding velocity $\dot{x}$, and it is commonly constant in absence of viscous friction (see CSV model). This model has two drawbacks: I) it features a discontinuity at null velocity, and II) only viscous friction is present when normal force F_n is equal to zero. To get rid of both drawbacks, such a model can be rewritten as follows:

$$F_f = (\mu_d F_n + \mu_{d1})\tanh(k\dot{x}) + (\mu_f + \mu_{f1} F_n)\dot{x}. \quad (5)$$

This new formulation allows removing the aforementioned discontinuity by means of the hyperbolic tangent function replacing the sign function. The hyperbolic tangent yields a smoothed trend at very low velocities; a similar result can be obtained with several functions, e.g. exponential [10] Moreover, (5) introduces two more coefficients μ_{d1} and μ_{f1} such that the F_f has not only a viscous term when the applied normal force is equal to zero. In the next Section, results will highlight the enhanced performance of this modified version of the CV model. F_n is considered to coincide with the output of the load cell for all the models.

B. Karnopp Model

The Karnopp model was conceived with the aim of resolving the discontinuity of the Coulomb model for $\dot{x} = 0$. It introduces an interval $|\dot{x}| < V$ in which the velocity is assumed to be null. Within this interval, the Karnopp model accounts for stiction [10]. The formulation is not so different from the Coulomb model, though viscosity is generally neglected:

$$F_f = \begin{cases} (\mu_d F_n + \mu_{d1})\text{sign}(\dot{x}) & |\dot{x}| > V \\ \min(F, \mu_s F_n)\text{sign}(F) & |\dot{x}| \leq V. \end{cases} \quad (6)$$

Again, a further coefficient μ_{d1} is added. The stiction is modelled for velocities lower than the threshold V through the static coefficient of friction μ_s.

C. Threlfall Model

The Threlfall model uses an exponential function to avoid the discontinuity in the vicinity of null velocity. It is defined in this manner:

$$F_f = \begin{cases} (\mu_d + \mu_{d1} F_n)(1 - e^{-3|\dot{x}|/v_e})\text{sign}(\dot{x}) & |\dot{x}| \leq v_e \\ 0.95(\mu_d + \mu_{d1} F_n)\text{sign}(\dot{x}) & |\dot{x}| > v_e. \end{cases} \quad (7)$$

Interestingly, the exponential function confers this model a soft transition form positive to negative velocities. This characteristic makes redundant the use of function such as the hyperbolic tangent; the original function $\text{sign}(\dot{x})$ might be maintained, as for the Karnopp model. The transition around the null velocity is defined in the band $[-v_e, +v_e]$, i.e. where

the exponential function works. Indeed, when the absolute value of the velocity $|\dot{x}|$ equals v_e, the value of the term $(1 - e^{-3|\dot{x}|/v_e})$ approximates 0.95. Hence, F_f is defined as in the second equation of (7).

D. CVS Model

The CV model can be enriched inserting a mathematical description of the stick-slip. This phenomenon induces the friction force to vary with velocity in a non-linear fashion. The Stribeck friction offers a good solution for modelling such a phenomenon [3]. Plus, it creates a continuous transition from the stiction regimen to the Coulomb friction [2]. An analytical representation of the overall model including stiction, viscosity and stick-slip might be given by:

$$F_f = (\mu_d F_n + \mu_{d1})(1 - e^{-(v/v_s)^2})\tanh(k\dot{x}) + (\mu_s F_n + \mu_{s1})e^{-(v/v_s)^2}\tanh(k\dot{x}) + (\mu_f + \mu_{f1}F_n)\dot{x}. \quad (8)$$

Here, we replaced $\mathrm{sign}(x)$ with $\tanh(\dot{x})$ as for the CV model. Another solution is to combine the Stribeck friction with the Karnopp model to solve the discontinuity at null velocity [11]-[12]. The parameter v_s denotes the Stribeck velocity, and determines how fast will be the stiction-Coulomb transition. The higher v_s will be, the shorter will be such a transition. The Stribeck effect was found to be very accurate for approximating friction at low velocity [12].

IV. Experimental Tests and Results

In this Section, the identification experiments that were carried out will be shown together with the results.

A. Experiments and Identification Procedure

The experiments to identify the parameters of the four models were conducted at constant velocity. In more detail, the following tests were carried out on the pneumatic gripper:

- **force-controlled ramps, 0-30 N**: low velocity at 0.25 mm/s, 0.5 mm/s, 1.25 mm/s;
- **force-controlled ramps, 0-60 N**: low velocity at 0.5 mm/s, 1 mm/s, 2.5 mm/s;
- **force-controlled ramps, 0-60 N**: high velocity at 5 mm/s, 10 mm/s, 12.5 mm/s;
- **position-controlled ramps, 0-3 mm**: low velocity at 0.3 mm/s, 0.5 mm/s 1 mm/s.

The force-controlled tests were carried out on the *spring* setup, whereas for the position-controlled tests the *no-spring* setup was used. For all the force-controlled tests, the theoretical velocity was calculated by setting a given duration of the test. Therefore, by commanding the gripper to reach a desired force level (corresponding to a known stroke) in a certain time interval, velocity could be retrieved. Two desired force levels were applied for the force-controlled, low-velocity tests: 30 N and and 60 N, generating a stroke of 1.25 mm and 2.5 mm ca., respectively.

A pair of ramps, i.e. one for closing and the other one for opening the gripper, was repeated three times for all the force-controlled tests and one time for the position-controlled tests. During the latter, the gripper was commanded to move 3 mm in a fixed time interval. An example of force-controlled ramp is illustrated in Fig. 4. It can be observed that the gripper closes rather easily (left ramp), whereas it remains blocked when the force controller imposes an inverse ramp (right ramp). Furthermore, the gripper cannot completely reopen as a force offset is visible at the end of the trial (Time=10 s).

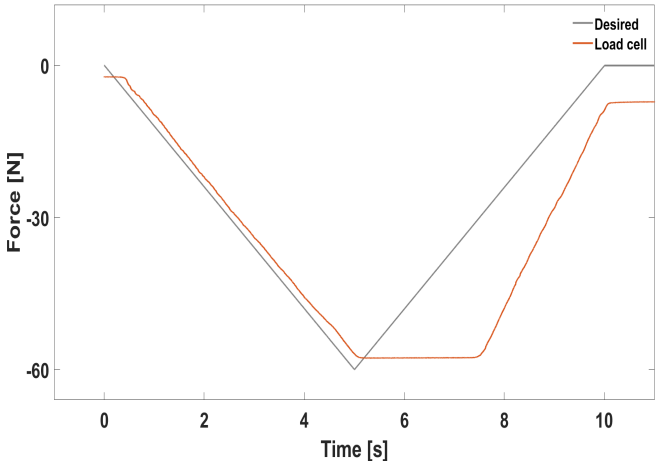

Fig. 4. Force-controlled ramp.

To identify the parameters of all the models, the same procedure was employed. First, the friction force F_{fexp} was retrieved from the experimental data:

$$F_{fexp} = F_p - F_m - F_i, \quad (9)$$

where F_p denotes the piston force actuating the gripper jaws (hence, the fingers) and F_m is the force measured by the load cell (assumed to coincide with F_n). The inertial force F_i could be neglected, being the experiments done at constant velocity. In any case, the contribution of this force is very low, being the mass of the moving parts (fingers, load cell and jaws) very little. The force balance in (9) can be expressed as:

$$F_{fexp} = |A_o \quad A_c||P_o \quad P_c|^T - F_m, \quad (10)$$

being the piston force F_p written as the difference between the pressures P_o and P_c, multiplying the relevant chamber areas A_o and A_c (a priori known from the gripper CAD model).

The identification procedure was the same for all the models. Once that F_{fexp} was found, the parameters to be identified were stacked in a vector I_p and obtained as follows:

$$I_p = E^{\dagger} F_{fexp}, \quad (11)$$

where E is the matrix containing the vectors which were functions either of F_m or $\dot{x}$, or even of both. For instance, (11) for the CV model had this form:

$$|\mu_d \quad \mu_{d1} \quad \mu_f \quad \mu_{f1}|^T = |\tanh(k\dot{x})F_n \quad \tanh(k\dot{x}) \quad \dot{x} \quad F_n\dot{x}|^{\dagger} F_{fexp}. \quad (12)$$

It is worth mentioning that some of the parameters were empirically estimated, i.e. the threshold V of the Karnopp model, the velocity v_e of the Threlfall model and the Stribeck velocity v_s. A very narrow band was defined for the Karnopp model by setting V to 0.2 mm/s, which was the same value found for v_s. v_e was 0.5 mm/s in the Threlfall model. The velocity $\dot{x}$ was calculated by differentiating the filtered position measured by the laser sensor. The applied filter was an exponential smoothing function with low-pass action.

B. Results

Fig. 5 depicts the friction force F_{fexp} vs the measured position, for the force-controlled experiments. The variation of the friction force is linear, as expected from constant velocities and from the presence of the spring governed by a linear force-position law. Moreover, stiction is evident at the beginning of the trials as a non-null force exists when the gripper is not yet able to move. As for the load cell, the laser sensor output was negative. Hence, decreasing position along with negative friction force corresponds to the gripper closing action; vice versa, the gripper opening is associated with increasing position and positive friction force.

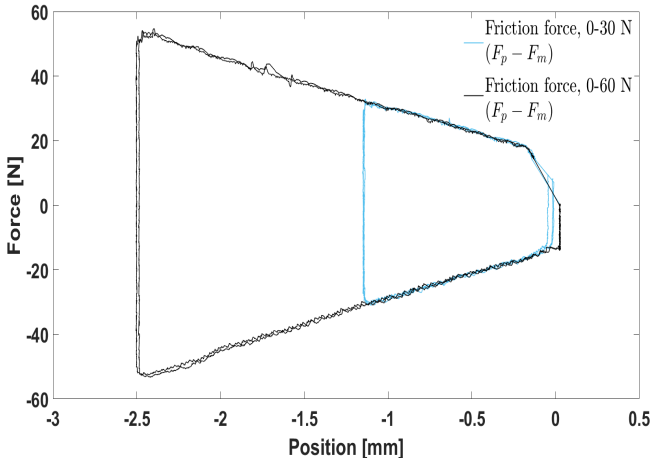

Fig. 5. Friction force F_{fexp} vs position.

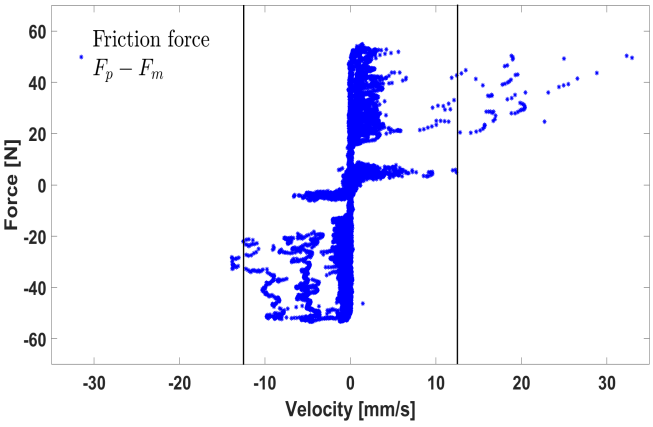

Fig. 6. Friction force F_{fexp} vs velocity.

Fig. 6 depicts the friction force F_{fexp} vs the velocity from all the experiments. Within the maximum theoretical velocities, i.e. $\pm 12.5 mm/s$, the force F_{fexp} manifests a behavior in line with the classic Coulomb model. Outside this region, viscosity seems to arise, even though very few data points are available (0.1%). Note that these points appear almost only when velocity is positive, i.e. when the gripper is reopening. In this phase, spurious accelerations might take place due to the higher difficulty met by the gripper to move, as also shown in Fig. 4.

The CV model is plotted in Fig. 7 without μ_{d1} and μ_{f1} (panel A), i.e. in its canonical form although smoothed by means of the $\tanh(k\dot{x})$ function. One can see that viscosity dominates in the CV model if the viscous friction is expressed through the mere μ_f and only dependence on the velocity $\dot{x}$ is expressed. As a consequence, the so formulated model fails to predict friction on the collected dataset. Removing viscosity, i.e. setting μ_f to zero does not improve the prediction, even reintroducing μ_{d1} in the Coulomb friction (panel B).

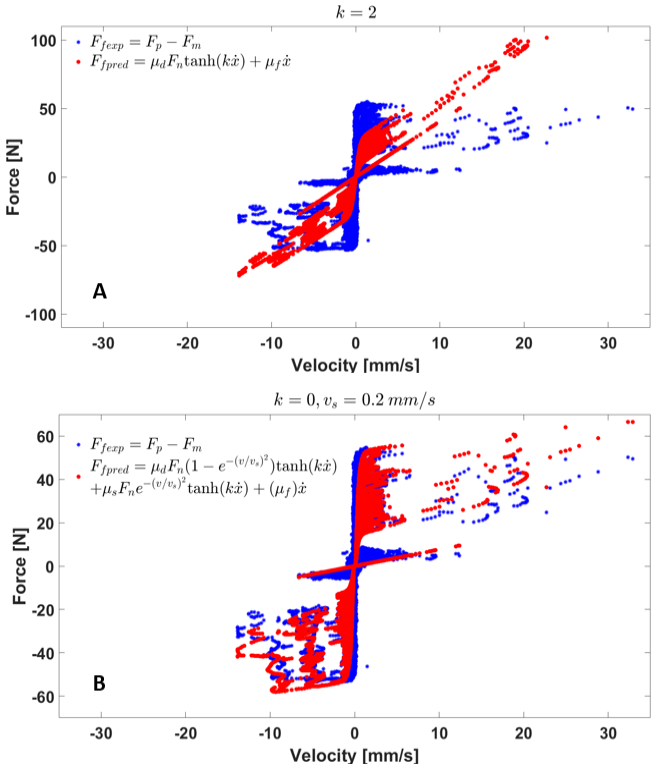

Fig. 7. Friction force F_{fpred} predicted by the CV model with classic definition (panel A) and without viscosity (panel B).

Considering instead the definitions of (5), (6), (7) and (8), the results of the identification are shown in Fig. 8. All the models reproduce the behavior of the real friction force F_{fexp} in an acceptable manner. The most accurate model is the CSV one, with a mean error of just 0.115 N. This is evident from the plot, as the CSV is the only model featuring a precise fit even for the spurious data points outside the region delimited by the maximum theoretical

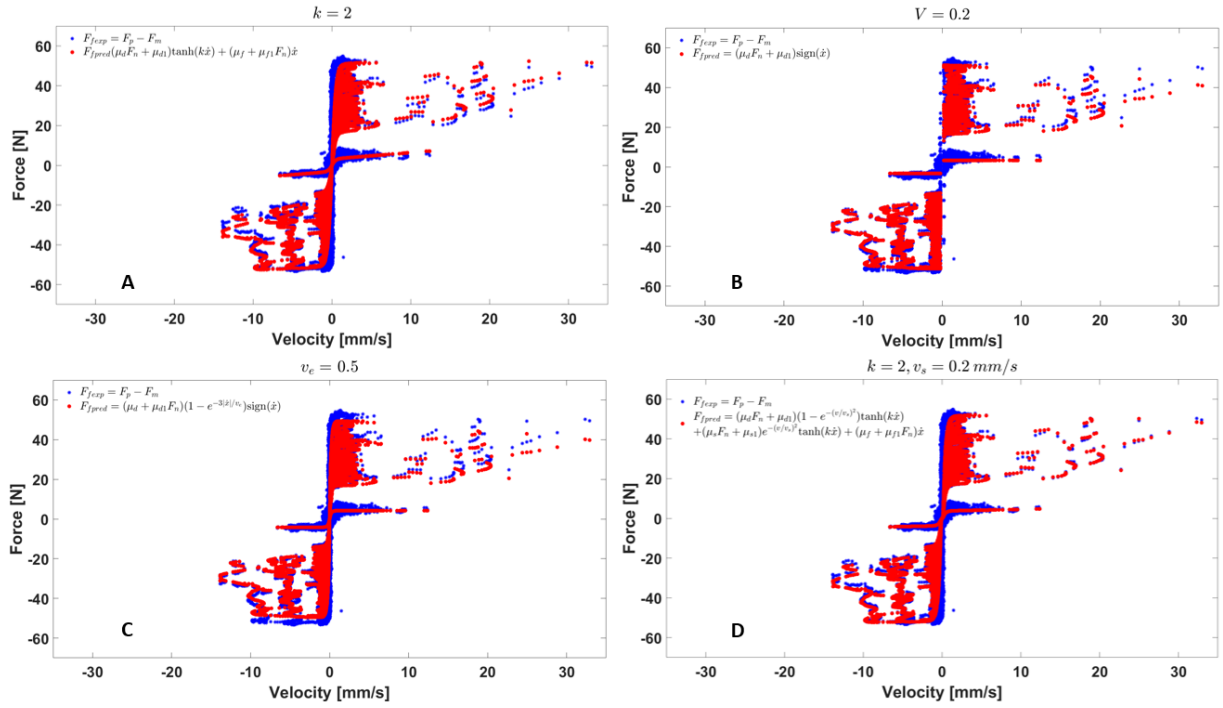

Fig. 8. Prediction of the friction models. A: CV model, B: Karnopp model, C: Threlfall model, D: CSV model.

velocities. Further, the CV model offers high accuracy being its mean error as low as 0.205 N. Karnopp and Threlfall models seem to slightly underestimate the friction force at high values, i.e. close to 60 N. Their prediction tends to diverge as velocity increases. Nonetheless, mean error is 0.508 N and 0.983 N, respectively. All the models appear reliable, as the mean error is lower than 1 N in all cases. Intuitively, the models performing best are the ones with more parameters.

V. CONCLUSIONS

In this work, we evaluated the performance of four friction models on a pneumatic gripper. The models were modified w.r.t. their classical definition so as to study their performance. Some experiments were carried out in order to acquire the data to be employed for the models identification. The gripper was mounted in two different setups and controlled both in force and position at different constant velocities. Results revealed that all the four models can predict with good accuracy the friction force retrieved from the experimental data. The most precise models are also the most complex ones, i.e. the ones with the highest number of parameters.

In future work, effort will be spent on investigating more models, such as dynamic models (e.g. the LuGre model). Experiments at non-constant velocity will be carried out so as to include the inertial force in the friction analysis. Furthermore, the investigated models will be integrated in closed-loop control architectures to compensate friction online, during the gripper operation.

REFERENCES

[1] C. C. De Wit, H. Olsson, K. J. Astrom, and P. Lischinsky, "A new model for control of systems with friction," *IEEE Transactions on automatic control*, vol. 40, no. 3, pp. 419–425, 1995.

[2] F. Marques, P. Flores, J. P. Claro, and H. M. Lankarani, "A survey and comparison of several friction force models for dynamic analysis of multibody mechanical systems," *Nonlinear Dynamics*, vol. 86, no. 3, pp. 1407–1443, 2016.

[3] B. Armstrong-Helouvry, "Stick-slip arising from stribeck friction," in *Proceedings., IEEE International Conference on Robotics and Automation*. IEEE, 1990, pp. 1377–1382.

[4] R. Beerens, A. Bisoffi, L. Zaccarian, W. Heemels, H. Nijmeijer, and N. van de Wouw, "Reset integral control for improved settling of pid-based motion systems with friction," *Automatica*, vol. 107, pp. 483–492, 2019.

[5] D. Karnopp, "Computer simulation of stick-slip friction in mechanical dynamic systems," 1985.

[6] D. Threlfall, "The inclusion of coulomb friction in mechanisms programs with particular reference to dram au programme dram," *Mechanism and Machine Theory*, vol. 13, no. 4, pp. 475–483, 1978.

[7] R. A. Romeo, L. Fiorio, E. J. Avila-Mireles, F. Cannella, G. Metta, and D. Pucci, "Closed-loop force control of a pneumatic gripper actuated by two pressure regulators," in *2019 IEEE/RSJ International Conference on Intelligent Robots and Systems (IROS)*. IEEE, 2019, pp. 7157–7162.

[8] X. Tran, H. Dao, and K. Tran, "A new mathematical model of friction for pneumatic cylinders," *Proceedings of the Institution of Mechanical Engineers, Part C: Journal of Mechanical Engineering Science*, vol. 230, no. 14, pp. 2399–2412, 2016.

[9] R. Romeo, L. Fiorio, G. L'Erario, M. Maggiali, G. Metta, and D. Pucci, "Dynamic control of a rigid pneumatic gripper," *IEEE Robotics and Automation Letters*, vol. PP, pp. 1–1, 02 2020.

[10] E. Pennestrì, V. Rossi, P. Salvini, and P. P. Valentini, "Review and comparison of dry friction force models," *Nonlinear dynamics*, vol. 83, no. 4, pp. 1785–1801, 2016.

[11] Z. Situm, D. Pavkovic, and B. Novakovic, "Servo pneumatic position control using fuzzy pid gain scheduling," *J. Dyn. Sys., Meas., Control*, vol. 126, no. 2, pp. 376–387, 2004.

[12] H. Feng, W. Qiao, C. Yin, H. Yu, and D. Cao, "Identification and compensation of non-linear friction for a electro-hydraulic system," *Mechanism and Machine Theory*, vol. 141, pp. 1–13, 2019.